Clim Dyn (2009) 32:887–900
DOI 10.1007/s00382-008-0424-4

A new framework for isolating individual feedback processes in coupled general circulation climate models. Part II: Method demonstrations and comparisons

Ming Cai · Jianhua Lu

Received: 14 November 2007 / Accepted: 14 May 2008 / Published online: 12 June 2008

Abstract We here use a coupled atmosphere-surface single column climate model to illustrate how the CFRAM, a new climate feedback analysis framework formulated in Part I of the two-part series papers, can be applied to isolate individual contributions to the total temperature change of a climate system from the external forcing alone, and from each of individual physical and dynamical processes associated with the energy transfer with the space and within the climate system. We demonstrate that the isolation of individual feedbacks in the CFRAM is achieved without referencing to a virtual climate system as in the online feedback suppression method. We show that partial temperature changes estimated by the online feedback suppression method include the "compensating effects" of other feedbacks when the feedback under consideration is suppressed. The partial temperature changes are addable in the CFRAM but they are not in the online feedback suppression method. We also apply the CFRAM to isolate the contributions to the lapse rate feedback from individual physical and dynamical feedback processes. We show that the lapse rate feedback includes not only the partial effect of each feedback that directly contributes to energy flux perturbations at the TOA (such as water vapor feedback), but also the total effects of those feedbacks that do not contribute to energy flux perturbations at the TOA (such as evaporation and moist convection feedbacks). Because the contributions to the lapse rate feedback from various physical and dynamical processes tend to cancel one another, the net lapse rate feedback is a residual of many large terms. This leads to a large uncertainty not only in estimating the lapse rate feedback itself, but also in other feedbacks whose effects are either partially or totally lumped into the lapse rate feedback.

M. Cai (✉) · J. Lu
Department of Meteorology, Florida State University, Tallahassee, FL 32306, USA
e-mail: cai@met.fsu.edu

1 Introduction

In Part I of the two-part series papers (Lu and Cai 2008, referred to as Part I hereafter), we formulated a new climate feedback analysis framework, referred to as the coupled atmosphere-surface "*c*limate *f*eedback-*r*esponse *a*nalysis *m*ethod" (abbreviated as "CFRAM"). The formulation of the CFRAM is based on the energy balance in both the atmosphere and the land/ocean column underneath. We take advantage of the fact that the infrared radiation is explicitly and directly related to temperatures in the entire atmosphere-surface column. Therefore, the temperature change in the equilibrium response to a non-temperature induced radiative energy flux perturbation (i.e., due to anthropogenic greenhouse gases or due to a change in water vapor, cloud, and surface albedo) or a non-radiative energy flux perturbation (i.e., due to a change in surface turbulent energy flux, in vertical- and horizontal-energy transport) can be uniquely determined by requiring the corresponding change in the infrared radiation to exactly balance the energy flux perturbation under consideration. In the CFRAM, the isolation of partial temperature changes due to individual feedbacks is achieved by solving the linearized infrared radiation transfer model subject to individual perturbations. The decomposition of feedbacks is based on the thermodynamic and dynamical processes that directly represent individual energy flux terms. The isolated partial temperature changes due to the external forcing alone or due to

each of the feedbacks are additive and their sum is the total response of the climate system to the external forcing.

In Part II of the two-part series papers, one of our two primary objectives is to demonstrate how to apply the CFRAM for diagnosing climate feedbacks in the context of global warming simulations using a coupled atmosphere-surface single column climate model. The procedures reported here can be easily adopted for climate feedback analysis using outputs of coupled general circulation models (CGCMs). The other main objective of this paper is to compare the results of climate feedback analysis using the CFRAM with those obtained with the "partial radiative perturbation" method (PRP, Wetherald and Manabe 1988) and with the online feedback suppression method (Hall and Manabe 1999; Schneider et al. 1999) to illustrate and understand the differences in these climate feedback analysis methods from the CFRAM perspective. Readers may consult with Bony et al. (2006) for a thorough review on the strengths and limitations of the PRP and online feedback suppression methods.

It should be pointed out that we could apply the CFRAM to diagnose the climate sensitivity using the outputs of IPCC AR4 climate model simulations. For example, we can estimate the partial temperature changes due to the external forcing alone, due to water vapor feedback, due to surface albedo changes, due to changes in surface sensible and latent heat fluxes since the data required for the calculations are readily available (e.g., http://www-pcmdi.llnl.gov/ipcc/about_ipcc.php). However, other data outputs required for a complete climate feedback analysis using the CFRAM, such as the dynamic heating fields associated with both convection and horizontal energy transport by large scale motions, and 3-D daily cloud fields, are not currently provided or archived by climate research centers. As a result, we could not illustrate how these partial temperature changes due to the external forcing alone, and due to all individual feedbacks can be added up and then compare the sum of all of these partial temperature changes with the total temperature change recorded in the original climate simulations. This is the primary reason that prompts us to use a simple coupled atmosphere-surface single column climate model. As to be shown shortly, by archiving all required fields from the outputs of the climate model, we can demonstrate that the partial temperature changes due to the external forcing alone and due to all feedbacks calculated by the CFRAM indeed are addible and the sum of them can be directly compared with the total temperature changes in the original climate simulations. We believe that the procedures illustrated here can be easily used to evaluate the partial contributions to total temperature change from each energy transfer and transport process in the context of coupled general circulation models with a full physical parameterization package provided that the required data outputs are readily available.

The organization of the presentation is as follows. Section 2 describes briefly the coupled atmosphere-surface single column climate model used in this study. Presented in Sect. 3 are the results of climate feedback analysis with the CFRAM method using the outputs of global warming simulations made with the simple climate model. In Sect. 3, we also discuss the accuracy of the CFRAM calculations. Section 4 is devoted to a comprehensive one-to-one comparison between the CFRAM and online feedback suppression method whereas Sect. 5 discusses the difference between the CFRAM and PRP methods. Section 5 also discusses the isolation of the contributions to the lapse rate feedback from each of individual physical and dynamical feedbacks. A brief summary about the main findings of this paper is provided in Sect. 6.

2 The coupled atmosphere-surface single column climate model

The coupled atmosphere-surface single column climate model consists of an atmospheric radiative-convective model coupled with a simple surface energy balance model that exchanges energy with the atmosphere though radiation, and sensible and latent heat fluxes. The radiative transfer component of the radiative-convective model is the radiative transfer model reported in Fu and Liou (1993). The same vertical profile of the atmospheric relative humidity used in Manabe and Wetherald (1967) is specified in both the standard CO_2 (330 ppm, denoted as ("$1 \times CO_2$") and the doubling CO_2 (660 ppm, denote as "$2 \times CO_2$") climate simulations. The ozone vertical profile used in the radiative transfer model is taken from the climatological ozone values in the tropics (Fu, personal communication). We use the standard concentration values of other greenhouse gases, such as CH_4 and NO_2, specified in the original radiative transfer model (Fu and Liou 1993). For the simplicity, we here do not consider effects of clouds and change in the surface albedo (the surface albedo has a fixed value of 0.3).

To mimic the moist convection process in the atmosphere, the latent heat entering the atmosphere through the surface latent heat flux is assumed to be instantaneously released with a vertical profile of condensation rate specified according to

$$\frac{dP}{dp} = \begin{cases} \frac{3E}{4\Delta p}\left[1 - \frac{(p-p_{\mathrm{mid}})^2}{(\Delta p)^2}\right] & \text{for } p_{\min} \le p \le p_{\max} \\ 0 & \text{otherwise} \end{cases} \quad (1)$$

where p is pressure level; E is the surface evaporation rate; P is the condensation rate at level p; $p_{\min} = 292$ hPa, $p_{\max} =$

831 hPa, $p_{\text{mid}} = (p_{\min} + p_{\max})/2$, and $\Delta p = (p_{\max} - p_{\min})/2$. It is easy to verify that the vertical integration of the condensation rate in (1) is exactly equal to the evaporation rate. According to (1), the condensation only takes place between $p_{\min}$ and $p_{\max}$ and the maximum latent heat is released at p_{mid} (about 560 hPa). The same vertical distribution of the latent heat per unit of the surface evaporation rate is used in both 1 × CO_2 and 2 × CO_2 climate simulations. Also a dry-convective adjustment scheme is added to the radiative-transfer model to mimic the dry convection that keeps the atmospheric lapse rate from exceeding 6.5 K/km in both 1 × CO_2 and 2 × CO_2 climate simulations.

The atmosphere is divided into 43 layers. There are 22 layers in the troposphere (between 1,000 and 100 hPa) and the remaining 21 layers in the stratosphere (above 100 hPa). The top layer of the atmosphere is labeled as layer 1 and the bottom layer is 43. The surface layer is labeled as the 44th layer of the coupled atmosphere-surface model. When the solution of the coupled atmosphere-surface global climate model reaches its equilibrium state, the energy balance of the atmosphere-surface system is

$$\underbrace{\begin{pmatrix} R_1 \\ \vdots \\ R_{43} \\ R_{44} \end{pmatrix}}_{\vec{R}} = \underbrace{\begin{pmatrix} S_1 \\ \vdots \\ S_{43} \\ S_{44} \end{pmatrix}}_{\vec{S}} + \underbrace{\begin{pmatrix} Q_1^{drv} \\ \vdots \\ Q_{43}^{drv} \\ 0 \end{pmatrix}}_{\vec{Q}_{\text{dry}}} + \underbrace{\begin{pmatrix} LP_1 \\ \vdots \\ LP_{43} \\ -LE \end{pmatrix}}_{\vec{Q}_{lh}} + \underbrace{\begin{pmatrix} 0 \\ \vdots \\ H \\ -H \end{pmatrix}}_{\vec{Q}_{sh}} \tag{2}$$

where elements in $\vec{\mathbf{R}}$ is the energy flux vector whose elements are the net infrared radiation flux leaving the mth layer atmosphere for $m = 1, 2, \ldots, 43$ and the net infrared radiation leaving the surface layer for $m = 44$; S_m in $\vec{\mathbf{S}}$ is the solar radiation flux absorbed by the mth layer atmosphere for m × 43 and S_{44} solar radiation flux absorbed at the surface; $\vec{\mathbf{Q}}^{\text{dry}}$ is the vertical profile of the dynamic heating rate calculated from the dry-convective adjustment scheme that helps to keep the atmospheric lapse rate not greater than 6.5 K/km. $Q_{44}^{lh} = -\text{LE}$ in $\vec{\mathbf{Q}}^{lh}$ is the surface latent heat flux and the remaining elements are the atmospheric condensation heating rate LP_m (m = 1, 2, …, 43) whose vertical profile is specified according to (1) and satisfies $\text{LE} = L\sum_{m=1}^{43} P_m$ (L is the latent heat constant); All elements in $\vec{\mathbf{Q}}^{sh}$ are zero except at the bottom layer of the atmosphere and the surface layer, representing heat exchange between the atmosphere and surface through the surface sensible heat flux H. It is of importance to remind here that all terms in (2) have a unit of Wm^{-2} and that the values of elements of $\vec{\mathbf{R}}$ can be changed only through changes in CO_2, q (atmospheric specific humidity), and T (atmospheric and surface temperatures) because the concentration level of the other gases is kept constant and the effects of clouds are not considered in this simple model.

The surface sensible and latent heat fluxes are determined according to

$$H = \alpha(T_{44} - T_{43}) \text{ and } E = \beta[q_s(T_{44}) - r_{43}q_s(T_{43})] \tag{3}$$

where $\alpha = 3\ \text{Wm}^{-2}\ \text{K}^{-1}$; $\beta = 0.003\ \text{kgs}^{-1}$; T_{44} and T_{43} are the surface and lowest atmosphere layer temperatures; r_{43} (=0.8) is the relative humidity at the lowest layer of the atmosphere; and q_s is the saturation specific humidity. Obviously, the energy balance equation (2) is a simplified version of the energy balance equation of the real climate system (e.g., Eq. (1) in Part I), but it includes sufficient elements for us to elucidate the principle of climate feedback analysis using the CFRAM.

Figure 1a, b shows the vertical profiles of temperature and specific humidity in the 1 × CO_2 equilibrium state of the coupled atmosphere-surface single column climate model obtained with a solar constant equal to 404 W/m^2 (an annual mean value in the tropics). The surface temperature of this model is about 293 K. The model's tropopause is at about 100 hPa. In the 1 × CO_2 equilibrium state, the surface latent heat flux is about 48.8 W/m^2 (upward, corresponding to a mean evaporation rate of 616 mm/year) and the surface sensible heat flux is 17.6 W/m^2 (upward), and the sum of the two exactly balances the net radiative flux of 66.4 W/m^2 entering the surface.

With interest of future application of the CFRAM in diagnosing the IPCC climate projection simulations, we consider the climate forcing due to the doubling of CO_2 in the model. It is seen that the largest radiative heating due to the doubling of CO_2 in the model is at the surface (about 1.5 W/m^2, Fig. 1c). In the atmosphere, the doubling of CO_2 yields a maximum radiative heating perturbation (about 1.18 W/m^2) at 800 hPa (or layer 41), but a cooling between 600 and 300 hPa. The radiative perturbation due to the doubling of CO_2 is positive but small between 300 and 150 hPa and is negative throughout the stratosphere.

The black curve in Fig. 2a represents the vertical profile of the (total) temperature change (the difference between the 2 × CO_2 and 1 × CO_2 equilibrium states) in response to the external forcing. The temperature change produced by this simple model yields a very familiar vertical pattern of global warming, namely, warming at the surface and in the troposphere but cooling in the stratosphere. The surface warming is 2.45 K. The tropospheric warming is slightly stronger than the surface warming (the mean warming between the surface and 200 hPa is about 2.7 K). The intensity of the stratosphere cooling increases with height. The cooling at 20 hPa is about −6 K in this model.

Obviously, the magnitude of the surface warming produced by this simple coupled atmosphere-surface climate

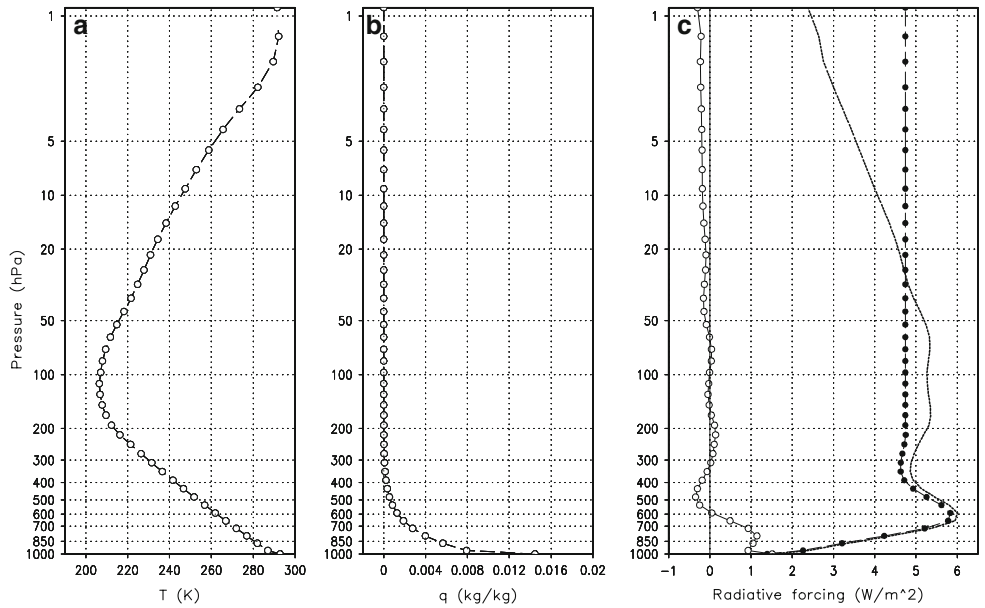

Fig. 1 **a** Vertical profile of the equilibrium temperature (K) in the standard 1 × CO_2 simulation using the coupled atmosphere-surface single column climate model. **b** The same as **a** except for the specific humidity (kg/kg). **c** Vertical profiles of radiative flux perturbation (W/m^2) due to the doubling of CO_2. *Open circles* the net radiative energy flux perturbation in each layer (positive for heating rate and negative for cooling rate) calculated using (5), *dashes* the net downward radiative energy flux perturbation which is the vertical integration of the red curve from the surface. *Closed circles* the net downward radiative energy flux perturbation due to the doubling of CO_2 with stratospheric adjustment (Ramaswamy et al. 2001)

model (Fig. 2a) is in the lower end of the global warming projections made with the state-of-art coupled general circulation models (CGCMs). This could be partially attributed to the absence of the ice-albedo feedback in the simple climate model. However, the purpose here is not to attempt to replicate the great success of CGCMs in projecting future climate changes using this simple climate model. Instead, we here wish to demonstrate how to apply the CFRAM to calculate the partial temperature changes due to the external forcing alone and due to each of the feedbacks in the model.

3 Feedback analysis using the CFRAM

As discussed in Part I, the CFRAM is formulated by using the linearized radiative transfer model in the energy perturbation equation of a coupled atmosphere-surface climate system. Specifically, the perturbation equation of (2) with a linearized radiative transfer model is

$$\Delta\vec{\mathbf{T}} = \left(\frac{\partial\vec{\mathbf{R}}}{\partial\vec{\mathbf{T}}}\right)^{-1} \times \left\{\Delta\vec{\mathbf{F}}^{\text{ext}} + \Delta^{(w)}(\vec{\mathbf{S}} - \vec{\mathbf{R}}) + \Delta\vec{\mathbf{Q}}^{\text{dry}} + \Delta\vec{\mathbf{Q}}^{lh} + \Delta\vec{\mathbf{Q}}^{sh}\right\} \tag{4}$$

where $\left(\frac{\partial\vec{\mathbf{R}}}{\partial\vec{\mathbf{T}}}\right)^{-1}$ is the inverse of the Planck feedback matrix;$\Delta\vec{\mathbf{T}}$ denotes the (total) temperature change in the entire atmosphere-surface column in response to the external forcing $\Delta\vec{\mathbf{F}}^{\text{ext}}$ due to the doubling CO_2 in the model; $\Delta^{(w)}(\vec{\mathbf{S}} - \vec{\mathbf{R}})$is the energy flux perturbation due to water vapor feedback; $\Delta\vec{\mathbf{Q}}^{\text{dry}}$ is the energy flux perturbation due to atmospheric dry convection feedback; $\Delta\vec{\mathbf{Q}}^{lh}$ is the energy flux perturbation due to the surface latent heat flux feedback plus the parameterized simultaneous moisture convection with the prescribed vertical heating distribution according to (1); and $\Delta\vec{\mathbf{Q}}^{sh}$ is the energy flux perturbation due to the surface sensible heat flux feedback. Note there is no change in the solar energy because the model (2) does not have clouds and the surface albedo is fixed at 0.3.

The radiative forcing $\Delta\vec{\mathbf{F}}^{\text{ext}}$ (the curve with open circles in Fig. 1c) is obtained by

$$\Delta\vec{\mathbf{F}}^{\text{ext}} = -[\vec{\mathbf{R}}(2\times CO_2, q_{1\times CO_2}, T_{1\times CO_2}) - \vec{\mathbf{R}}(1\times CO_2, q_{1\times CO_2}, T_{1\times CO_2})] \tag{5}$$

where the subscript "1 × CO_2" denotes that the vertical profile of the corresponding variable is taken from the 1 × CO_2 equilibrium state of the full model (2). Similarly, the radiative energy flux perturbation $\Delta^{(w)}(\vec{\mathbf{S}} - \vec{\mathbf{R}})$ is obtained by

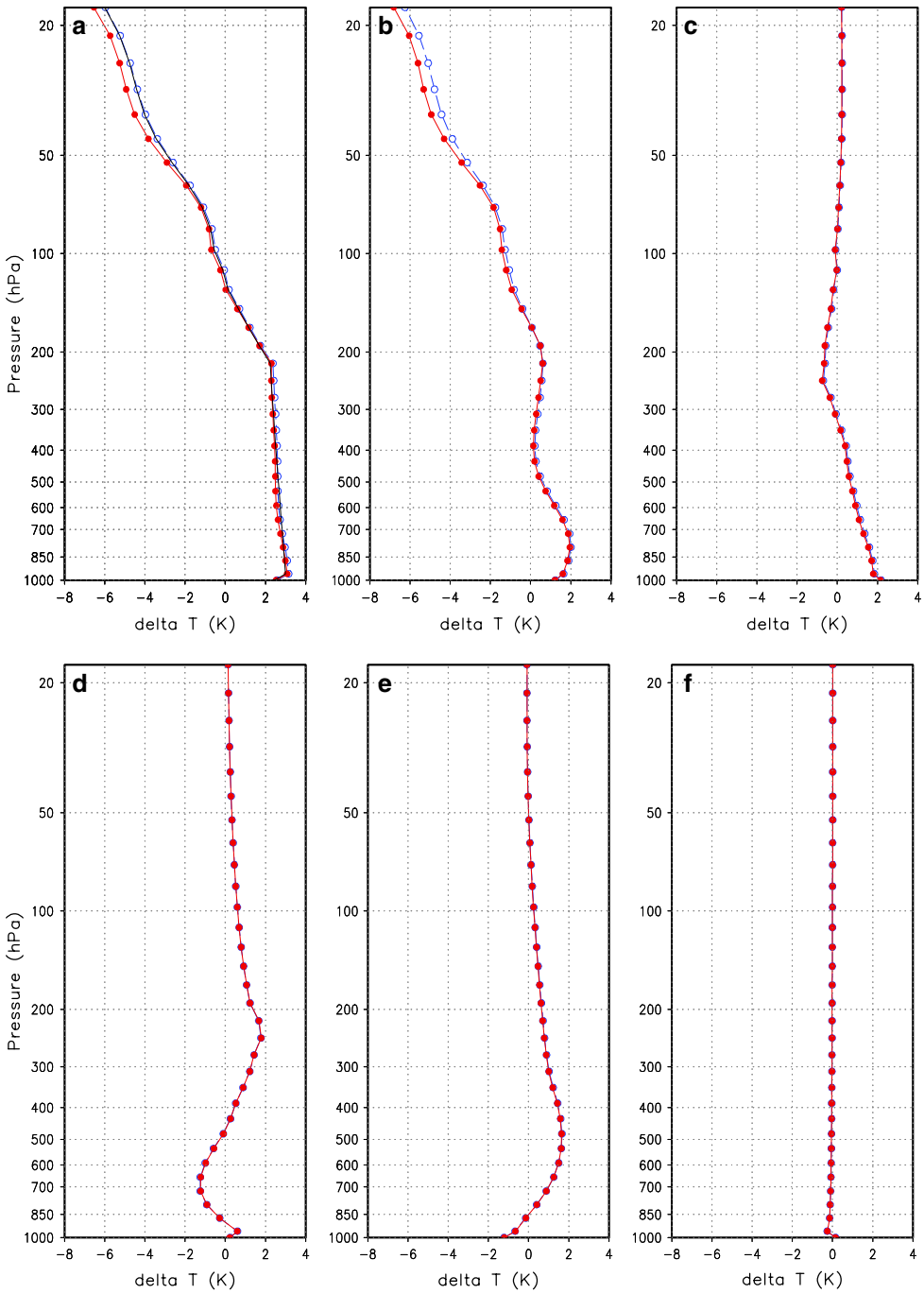

Fig. 2 Vertical profiles of temperature changes. **a** Total temperature change (*solid black curve* temperature difference between the 2 × CO_2 and 1 × CO_2 climate simulations, *red curve* sum of the red curves in **b**–**f**, *blue curve* sum of the blue curves in **b**–**f**. **b** Partial temperature change ($\Delta\bar{\mathbf{T}}^{ext}$) due to the external forcing alone (*red* CRFRAM calculation using (7); blue: nonlinear version of the CFRAM using (8)). **c** Same as **b** except for partial temperature change due to water vapor feedback ($\Delta\bar{\mathbf{T}}^{w}$). **d** Same as **b** except for partial temperature change due to changes in dry convection feedback ($\Delta\bar{\mathbf{T}}^{dry}$); **e** same as **b** except for partial temperature change due to changes in evaporation and moisture convection ($\Delta\bar{\mathbf{T}}^{lh}$); **f** same as **b** except for partial temperature change due to changes in surface sensible heat flux ($\Delta\bar{\mathbf{T}}^{sh}$)

$$\Delta^{(w)}(\vec{\mathbf{S}}-\vec{\mathbf{R}}) = [(\vec{\mathbf{S}}-\vec{\mathbf{R}})(1\times CO_2, q_{2\times CO_2}, T_{1\times CO_2}) - (\vec{\mathbf{S}}-\vec{\mathbf{R}})(1\times CO_2, q_{1\times CO_2}, T_{1\times CO_2})] \quad (6)$$

where the subscript "2 × CO_2" denotes that the vertical profile of the corresponding variable is taken from the 2 × CO_2 equilibrium state of the full model. Obviously, derivations of (5) and (6), as well as $\left(\frac{\partial\bar{\mathbf{R}}}{\partial\bar{\mathbf{T}}}\right)\Delta\bar{\mathbf{T}}$ in (4) are in accordance with the linearization of the radiative transfer model. The remaining three energy flux perturbation terms are obtained directly from their differences between the 2 × CO_2 and 1 × CO_2 equilibrium states without any linearization.

According to the CFRAM, the partial temperature changes due to the external forcing and these feedbacks can be directly calculated using

$$\Delta\vec{\mathbf{T}}^{ext} = \left(\frac{\partial\vec{\mathbf{R}}}{\partial\vec{\mathbf{T}}}\right)^{-1}\Delta\vec{\mathbf{F}}^{ext},\ \Delta\vec{\mathbf{T}}^{w} = \left(\frac{\partial\vec{\mathbf{R}}}{\partial\vec{\mathbf{T}}}\right)^{-1}\Delta^{(w)}(\vec{\mathbf{S}}-\vec{\mathbf{R}}),$$
$$\Delta\vec{\mathbf{T}}^{dry} = \left(\frac{\partial\vec{\mathbf{R}}}{\partial\vec{\mathbf{T}}}\right)^{-1}\Delta\vec{\mathbf{Q}}^{dry},\Delta\vec{\mathbf{T}}^{lh} = \left(\frac{\partial\vec{\mathbf{R}}}{\partial\vec{\mathbf{T}}}\right)^{-1}\Delta\vec{\mathbf{Q}}^{lh},$$
$$\Delta\vec{\mathbf{T}}^{sh} = \left(\frac{\partial\vec{\mathbf{R}}}{\partial\vec{\mathbf{T}}}\right)^{-1}\Delta\vec{\mathbf{Q}}^{sh} \quad (7)$$

The accuracy of these partial temperature changes due to the external forcing and feedbacks can be checked by comparing the sum of these partial temperature changes (red curve in Fig. 2a) with the total temperature change (black curve in Fig. 2a). It is seen that the two curves are very close to one another except a noticeable difference of a few degrees above 50 hPa. At the surface, the total surface warming estimated from the CFRAM is 2.53 K (Table 1) and its difference with the actual surface warming (2.45 K) derived from the full nonlinear model is only 0.08 K, less than 4%. This confirms that these partial temperature changes due to the external forcing and feedbacks diagnosed using (7) are indeed addable to the total change obtained from the original model.

The red curves displayed in the remaining panels of Fig. 2 correspond to the partial temperature changes due to the external forcing (Fig. 2b), water vapor feedback (Fig. 2c), dry-convection feedback (Fig. 2d), surface latent flux and moist convection feedbacks (Fig. 2e), and surface sensible heat flux feedback (Fig. 2f). It is seen that the stratospheric cooling is entirely due to the direct response to the doubling CO_2 (Fig. 2b), consistent with the negative external radiative forcing (cooling) there (Fig. 1c). The temperature change due to the doubling CO_2 alone only yields about 1.2 K warming at the surface and the maximum warming (about 2.1 K) due to the doubling CO_2 alone is at about 800 hPa, the same elevation where the positive external radiative forcing in the atmosphere is strongest (Fig. 1c). Water feedback adds another 2.15 K warming to the surface temperature (Fig. 2c and Table 1). The additional warming due to water vapor feedback is maximal at the surface and gradually decreases with height. The water vapor feedback causes a cooling temperature trend near the tropopause level (between 300 and 100 hPa). The stronger warming in the lower troposphere and weaker warming in the middle and upper troposphere due to the external forcing and water vapor feedback results in a stronger vertical (dry) convection in order to keep the tropospheric lapse rate not greater than 6.5 K/km as specified in our simple model. As a result, the feedback due to changes in dry convection acts to warm the mid-upper troposphere at an expense of reducing the warming in the lower troposphere (Fig. 2d). Although dry convection does not directly produce heating perturbation at the surface, the upper troposphere warming induced by its feedback still has a small influence on the surface warming through the back radiation effect (contributing about 0.23 K to the total surface warming, Table 1). The evaporation feedback causes a reduction of the surface warming by about 1.2 K in this model (Fig. 2e and Table 1) by evaporating more water from the surface. Then the enhanced hydrological cycle due to a stronger surface evaporation causes additional warming in the mid-upper troposphere through an increased condensation latent heating (Fig. 2e). Because of the reduction of the surface warming due to the evaporation feedback, the difference between the surface and surface air temperatures becomes smaller, leading to a small reduction of the surface sensible heat flux. The small reduction of the surface sensible heat flux results in a slight increase of the surface temperature at an expense of reducing the warming in the surface air temperature (Fig. 2f). Overall, the doubling of CO_2 and water vapor feedback are the main contributors to the surface warming in this simple climate model while the evaporation feedback dampens down the surface warming significantly. When the similar analysis using the CFRAM is applied to CGCM climate simulations, we would be able to relate the spatial pattern of global warming and the changes in energy cycle in the climate system.

Table 1 Surface temperature changes derived from the full model simulations, from the online feedback suppression simulations, from the CFRAM, and nonlinear version of the CFRAM

	ΔT_s^{ext}	ΔT_s^{w}	ΔT_s^{dry}	ΔT_s^{lh}	ΔT_s^{sh}	ΔT_s^{tot}
Full model solution	N/A	N/A	N/A	N/A	N/A	2.45 K
Feedback-suppression	N/A	1.40 K	−0.08 K	−0.32 K	0.03 K	N/A
CFRAM	1.21 K	2.15 K	0.23 K	−1.21 K	0.15 K	2.53 K
nl_CFRAM	1.23 K	2.18 K	0.23 K	−1.23 K	0.15 K	2.56 K

As mentioned earlier, the sum of the partial temperature changes calculated using the CFRAM is very close to the total temperature change throughout the troposphere, but becomes noticeably different from the total temperature change in the stratosphere. To investigate whether the source for such a noticeable difference in the stratosphere is from the linear approximations used in (2–7), we re-calculate the partial temperature changes due to the external forcing and due to feedbacks, without explicitly linearizing the radiative transfer model, according to (we referred to this as nonlinear CFRAM or nl_CFRAM, hereafter),

$$\Delta\hat{T}^{\text{ext}}(p) = \hat{T}^{\text{ext}}(p) - T_{1\times CO_2}(p),$$
where $\hat{T}^{\text{ext}}(p)$ is the solution of
$$\vec{R}(2\times CO_2, q_{1\times CO_2}, \hat{T}^{\text{ext}}) = \vec{R}(1\times CO_2, q_{1\times CO_2}, T_{1\times CO_2}) \quad (8.a)$$

$$\Delta\hat{T}^{w}(p) = \hat{T}^{w}(p) - T_{1\times CO_2}(p),$$
where $\hat{T}^{w}(p)$ is the solution of
$$(\vec{\mathbf{S}} - \vec{\mathbf{R}})(1\times CO_2, q_{2\times CO_2}, \hat{T}^{w}) = (\vec{\mathbf{S}} - \vec{\mathbf{R}})(1\times CO_2, q_{1\times CO_2}, T_{1\times CO_2}) \quad (8.b)$$

$$\Delta\hat{T}^{\text{dry}}(p) = \hat{T}^{\text{dry}}(p) - T_{1\times CO_2}(p),$$
where $\hat{T}^{\text{dry}}(p)$ is the solution of
$$\vec{\mathbf{R}}(1\times CO_2, q_{1\times CO_2}, \hat{T}^{\text{dry}}) = \vec{\mathbf{R}}(1\times CO_2, q_{1\times CO_2}, T_{1\times CO_2}) + \Delta\vec{\mathbf{Q}}^{\text{dry}} \quad (8.c)$$

$$\Delta\hat{T}^{lh}(p) = \hat{T}^{lh}(p) - T_{1\times CO_2}(p),$$
where $\hat{T}^{lh}(p)$ is the solution of
$$\vec{\mathbf{R}}(1\times CO_2, q_{1\times CO_2}, \hat{T}^{lh}) = \vec{\mathbf{R}}(1\times CO_2, q_{1\times CO_2}, T_{1\times CO_2}) + \Delta\vec{\mathbf{Q}}^{lh} \quad (8.d)$$

$$\Delta\hat{T}^{sh}(p) = \hat{T}^{sh}(p) - T_{1\times CO_2}(p),$$
where $\hat{T}^{sh}(p)$ is the solution of
where $\vec{\mathbf{R}}(1\times CO_2, q_{1\times CO_2}, \hat{T}^{sh}) = \vec{\mathbf{R}}(1\times CO_2, q_{1\times CO_2}, T_{1\times CO_2}) + \Delta\vec{\mathbf{Q}}^{sh}$ (8.e)

In (8), the symbol "^" is denoted for the solutions derived from the nl_CFRAM in order to distinguish them from those from the (linear) CFRAM. The other notations in (8) follow the same convention as in (5) and (6). It is straightforward to show that (7) can be obtained directly by linearizing $\vec{\mathbf{R}}$ and $(\vec{\mathbf{S}} - \vec{\mathbf{R}})$in (8) about the $1\times CO_2$ equilibrium state.

The partial temperature changes evaluated using (8) are plotted as the blue curves in Fig. 2b–f and their sum is plotted as the blue curve in Fig. 2a. It is seen that the sum of the partial temperature changes evaluated using (8) is nearly identical to the total temperature change throughout the entire atmosphere-surface column. It is very clear from Fig. 2c–f that the partial temperature changes due of the feedbacks calculated using the CFRAM is indistinguishable from those using (8) because the blue curves in Fig. 2c–f are completely covered by red curves. Therefore, the improvement by including nonlinearity in the radiative transfer model mainly results in a more accurate calculation of the partial temperature change in the stratosphere due to the doubling of CO_2 alone (blue versus red curves in Fig. 2b). The reason for the difference in the stratosphere between the CFRAM and nl_CFRAM can be attributed to the usage of the (linearized) Planck feedback matrix in the CFRAM. As shown in Fig. 1 of Part I, the diagonal elements of the Planck feedback matrix have smaller numerical values in the stratosphere (upper left corner in Fig. 1 of Part I). As a result, the linear solution (CFRAM) would be very sensitive to the forcing in the stratosphere, which is not the problem for the nl_CFRAM because it does not involve linearization of the radiative transfer model. Because the energy flux perturbations due to feedbacks are nearly absent in the stratosphere in this simple climate model, the partial temperature changes due to feedbacks calculated from the CFRAM seem indistinguishable from those using the nl_CFRAM. It is expected that the accuracy of the CFRAM in the stratosphere could be further improved by reducing number of computational layers in the stratosphere in the CFRAM calculations because this would increase the numerical values of the upper left corner of the Planck feedback matrix.

The results shown in Fig. 2 clearly illustrate that the CFRAM indeed enables us to calculate the partial temperature changes due to the climate forcing alone, and due to various feedbacks separately and the sum of the partial temperature changes is addable to the total response. Although the nonlinear version of the CFRAM can improve the accuracy in the stratosphere (mostly in the partial temperature change due to the climate forcing alone), the CFRAM is much cheaper (in terms of computational cost) and easier to use than the nl_CFRAM. Also, strictly speaking, the partial temperature changes calculated from the nl_CFRAM are not supposed to be addable. The fact that their sum is very close to the total change in this case implies that the nonlinear effect in the radiative transfer model is weak for a perturbation only as large as $2\times CO_2$ climate forcing.

4 Comparison with the online feedback suppression method

In the literature, the online feedback suppression method has been used to estimate mainly the partial temperature changes due to water vapor feedback in CGCMs (Hall and Manabe 1999; Schneider et al. 1999). Here, we have made four new doubling CO_2 experiments with the full model (2) and each of them suppresses only one of the four feedbacks considered in Fig. 2. The suppression is achieved by fixing the vertical profile of a variable that is responsible for the feedback to its profile in the $1\times CO_2$ equilibrium state (e.g., setting $X(p) = X_{1\times CO_2}(p)$where $X = q$ for water vapor feedback suppression, $X = Q^{\text{dry}}$ for dry convection feedback suppression, $X = Q^{lh}$ for evaporation and moist

convection feedback suppression, and $X = Q^{sh}$ for surface sensible flux feedback suppression). Then the difference between the original 2 × CO_2 state and the new 2 × CO_2 equilibrium state in which one feedback is suppressed corresponds to the partial temperature change due to that suppressed feedback.

Displayed in Fig. 3 are the partial temperature changes due to each of the four feedback processes calculated using the feedback-suppression method (green curves). For an easy comparison, the partial temperature changes calculated using the CFRAM shown in Fig. 2c–f are also presented in Fig. 3 (red curves). It is easy to see that there are some noticeable differences in the partial temperature changes calculated with the two methods. For example, the partial surface warming due to water vapor feedback is about 1.4 K according to the feedback-suppression method, noticeably smaller than that calculated using the CFRAM (2.15 K, Table 1). The largest difference in the partial temperature changes due to water vapor feedback between the two methods is in found in the upper troposphere (between 500 and 100 hPa) where the water vapor feedback induced partial temperature change obtained with the feedback-suppression method can be 2 K warmer than that calculated using the CFRAM.

The negative feedback to the surface temperature due to changes in evaporation estimated from the feedback-suppression method appears to be very weak, producing −0.32 K change in the surface temperature, which is about 4 times weaker than that estimated from the CFRAM (Table 1). The smaller increase of evaporation estimated by the feedback-suppression method is accompanied with a weaker intensification of moist convection, responsible for a smaller warming than that estimated in the CFRAM near 500 hPa where our specified latent heating profile reaches the maximum value (Fig. 3c). The weaker moist convection intensification estimated by the feedback-suppression method is also evident near the surface where the partial temperature change due to moist convection feedback estimated from the feedback-suppression method is positive, in contrary to the estimate made with the CFRAM. There are also noticeable differences in the estimates of the partial temperature changes due dry convection feedback made with these two methods (Fig. 3b). Although the feedback due to changes in surface sensible flux is small in this climate model, the estimate made from the feedback-suppression method is about five times smaller than that from the CFRAM (Fig. 3d and Table 1).

Now let turn attention on what are the main factors contributing the difference between the CFRAM and feedback suppression methods. By definition, the partial temperature change due to a particular feedback obtained by using the feedback-suppression method is the temperature difference between two different climate systems:

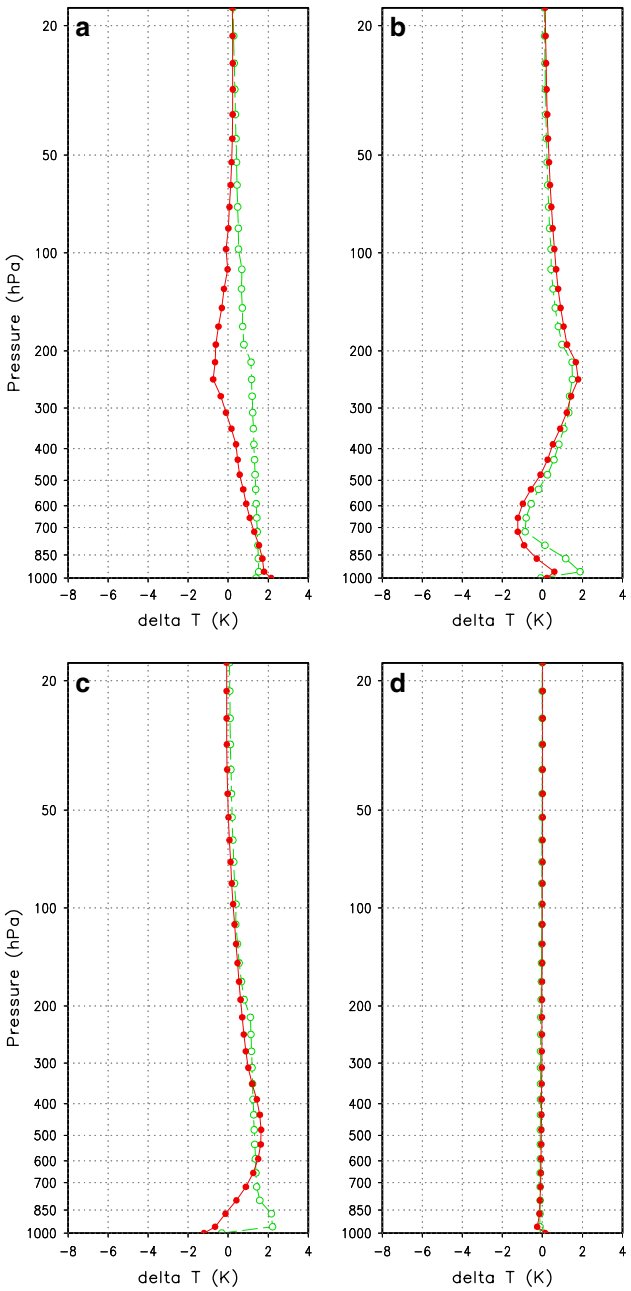

Fig. 3 Vertical profiles of partial temperature changes due to **a** water vapor feedback ($\Delta\bar{\mathbf{T}}^{w}$), **b** changes in dry convection ($\Delta\bar{\mathbf{T}}^{\mathrm{dry}}$), **c** changes in surface latent heat flux and moist convection ($\Delta\bar{\mathbf{T}}^{lh}$), and **d** changes in surface sensible heat flux ($\Delta\bar{\mathbf{T}}^{sh}$). *Red curves* for results calculated in the CFRAM and *green curves* for the results obtained from online feedback suppression climate simulations

one is the standard system with the presence of all feedbacks, and the other is a "virtual" system that include all feedbacks except the one under consideration. In this sense, the feedback-suppression measures the "inter-system" difference. On the contrary, the CFRAM does not rely on a

Table 2 Partial surface temperature changes calculated with the CFRAM using the outputs of the standard and water vapor-feedback-suppressed $2 \times CO_2$ simulations

	ΔT_s^{ext}(K)	ΔT_s^{w}(K)	ΔT_s^{other}(K)	$\Delta T_s^{ext}+\Delta T_s^{w}+\Delta T_s^{other}$(K)	ΔT_s(K)
A: Standard $2 \times CO_2$	1.21	2.15	−0.83	2.53	2.45
B: WV-feedback- suppressed $2 \times CO_2$	1.21	0.0	−0.17	1.04	1.05
A–B	0.0	2.15	−0.66	1.49	1.4

virtual climate system as a reference to infer the partial temperature change due to feedback processes. In this sense, the CFRAM analyzes the feedbacks that actually took place in the original climate system.

We now apply the CFRAM to diagnose the feedbacks that are not excluded in a feedback-suppression experiment to examine what cause the differences. Table 2 shows the results of using the CFRAM to calculate the contributions to the (total) surface temperature change from the external forcing and from feedbacks in both the standard $2 \times CO_2$ and water-vapor-feedback-suppressed $2 \times CO_2$ simulations. By the online feedback suppression alone, we only know that the (total) surface warming in the water-vapor-feedback-suppressed simulation is about 1.4 K less than that in the standard $2 \times CO_2$ simulation. By applying the CFRAM to both simulations, we wish to find out what contribute to the 1.4 K reduction of the surface warming in the water-vapor-feedback-suppressed simulation. Based on the CFRAM, the absence of the water vapor feedback would cause a reduction of the surface warming by 2.15 K. However, in the water vapor-feedback-suppressed $2 \times CO_2$ simulation, the effects of other feedbacks are also different from their counterparts in the standard $2 \times CO_2$ simulation. As indicated in Table 2, the difference in other feedbacks between the standard and feedback-suppression $2 \times CO_2$ simulations is −0.66 K. This accounts for the difference in estimating the partial temperature change due to water vapor feedback between the CFRAM and feedback suppression methods (2.15 K − 0.66 K = 1.49 K ≈ 1.4 K where the extra small difference 0.09 K is the error due to linearization approximation of the radiative transfer model in the CFRAM). Therefore, the difference between the CFRAM and feedback-suppression methods results from the "compensating" effects of the other feedbacks in the absence of the feedback that is purposely (but "artificially") suppressed. In the water-vapor-feedback-suppressed experiment, the absence of water vapor feedback attributes to a smaller warming at the surface and the smaller warming would then attributes to a smaller increase in evaporation, implying a smaller reduction of the surface warming by the evaporation feedback. Therefore, the compensating effect of the evaporation feedback in the feedback-suppressed experiments effectively attributes to a surface warming (by a less warming reduction) that partially cancels out the warming reduction due to the absence of the water vapor feedback alone. This results in a smaller estimation of the positive water vapor feedback to the surface warming by the online feedback suppression method. The same reduction of evaporation in the water-vapor-feedback-suppressed experiment also results in a reduction in warming atmosphere by the moist convection. This is the factor explaining why the online feedback suppression estimate a stronger positive water vapor feedback to the atmospheric warming, as indicated in Fig. 3a. Therefore, the difference between the online feedback suppression and CFRAM is entirely due to the compensating effects of other feedbacks in the climate system when one specific feedback is suppressed artificially.

In summary, the CFRAM is analog to the online feedback suppression method in that both of them are designed for estimation of the partial temperature changes, including their vertical and horizontal variations, due to individual feedback processes one by one. Obviously, in a linear system in which all physical processes that influence temperature are independent, the temperature change due to a specific feedback evaluated using the CFRAM would have to be identical to that inferred from the online feedback suppression method. For a nonlinear system such as the climate system, however, the feedbacks measured within the climate system as the case of the CFRAM are different from the "feedbacks measured in two different systems" as in the online feedback suppression method. In the online feedback suppression method, the difference between two different systems does not reflect exactly the actual effect of the suppressed feedback in the original climate system because the difference also includes the compensating effects from the other feedbacks. In other word, due to the interactions among various feedbacks, the strength of other feedbacks in the online feedback suppression experiment is different from the strength of the same feedbacks in the original climate system. As a result, the partial temperature change due to a specific feedback inferred by the online feedback suppression method also includes the difference in the other feedbacks between the original climate system and the virtual climate system. The feedback analysis based on the CFRAM does not need to introduce a (virtual) reference climate system. The

CFRAM does not cut each feedback under the consideration out of the nonlinear interactive loop with other feedbacks. The CFRAM can separate the individual contributions to the total temperature response change cleanly based on the outputs of a given climate perturbation simulation.

5 Comparison with the PRP method

Both CFRAM and PRP methods are offline and post-process diagnostic tools and they both are designed to diagnose feedbacks within the same climate system. As discussed in Part I, there are two fundamental differences between the CFRAM and PRP. One is due to the difference in the climate feedback-response definition and the other is due to the TOA-only approach versus the atmosphere-surface column approach. Sections 3 and 4 of Part I contain some lengthy discussions on these fundamental differences between the two methods, which are not repeated here. Below, we illustrate these differences by applying both methods for diagnosing climate feedbacks in the context of the coupled atmosphere-surface single column climate model.

5.1 Differences due to the difference in the definition of feedback-response

The differences between the CFRAM and PRP due to the difference in the climate feedback-response definition can be illustrated by comparing the TOA version of the CFRAM (TFRAM) with the PRP method. The feedback agents included in this simple single column climate model that can influence the TOA radiative energy fluxes are Planck feedback, lapse rate feedback, and water vapor feedback (they are denoted in the discussion below using subscripts/superscripts "P", "Γ", and "w", respectively).

As summarized in Table 3, the difference in the climate feedback-response definition results in two different sets of parameters measuring climate feedbacks and their effects although both methods use the same output data from the climate model simulations. With the PRP method, we calculate the following feedback parameters:

$$\lambda_P = -\sum_{m=1}^{44}\left(\frac{\partial R^{\mathrm{TOA}}}{\partial T_m}\right),\ \lambda_\Gamma = \sum_{m=1}^{44}\left(-\frac{\partial R^{\mathrm{TOA}}}{\partial T_m}\right)\frac{\Delta T_m - \Delta T_s}{\Delta T_s},$$
$$\lambda_w = \frac{\Delta^{(w)}(S-R)^{\mathrm{TOA}}}{\Delta T_s} \tag{9}$$

where $\frac{\partial R^{\mathrm{TOA}}}{\partial T_m}$ is the sum of all rows in the column "m" in the Planck feedback matrix $\left(\frac{\partial \bar{\mathbf{R}}}{\partial \bar{\mathbf{T}}}\right)$, and $R^{\mathrm{TOA}}$the net upward infrared radiation at the TOA; $\Delta^{(w)}(S-R)^{\mathrm{TOA}}$ is the sum of all rows in the vector $\Delta^{(w)}(\vec{\mathbf{S}}-\vec{\mathbf{R}})$ defined in (6); ΔT_m is the temperature change at the mth layer of the atmosphere-surface column derived from the difference between the $2\times CO_2$ and $1\times CO_2$ solutions of (2); $\Delta T_s = \Delta T_{44}$ is the surface temperature change. By PRP feedback definition, these feedback parameters are additive and their sum is the (total) feedback parameter of the model. The PRP initial gain is $G_0 = -1/\lambda_P$, and the total gain is $G = -1/(\lambda_P + \lambda_\Gamma + \lambda_w) = G_0/[1-(g_\Gamma + g_w)]$, where g_Γ and $g_w$are the PRP version of the gains of lapse rate and water vapor feedbacks, respectively. The values of these PRP feedback parameters and the initial and total gains are given in Table 3. Because the effects of the feedbacks based on the PRP are not addable, one cannot infer the partial temperature changes due to individual feedback agents. This feature is in accordance with the PRP feedback definition, which effectively views that all changes except the surface temperature are "feedback" responses to the change in the surface temperature and the surface temperature change is ultimately caused by the external forcing.

Table 3 Comparisons of feedback analysis using the PRP and TOA version of the CFRAM (TFRAM)

	PRP	TOA version of CFRAM
TOA forcing[a]	$\Delta F^{\mathrm{TOA}} = 4.74\mathrm{Wm}^{-2}$	ΔF^{TOA}= 4.74 Wm^{-2}
Initial gain	$G_0 = -1/\lambda_p = 0.257\ \mathrm{K/Wm}^{-2}$	$\tilde{G}_0 = -1/\lambda_p = 0.257\ \mathrm{K/(Wm}^{-2})$
Lapse rate feedback gain	$g_\Gamma = \lambda_\Gamma/(-\lambda_p) = -0.067$	$\tilde{g}_\Gamma = -0.131$
WV feedback gain	$g_w = \lambda_w/(-\lambda_p) = 0.586$	$\tilde{g}_w = 1.172$
Total gain	$G = G_0(1-g_\Gamma - g_w)^{-1} = 0.534\ \mathrm{K/(Wm}^{-2})$	$\tilde{G} = \tilde{G}_0(1+\tilde{g}_\Gamma + \tilde{g}_w) = 0.525\ \mathrm{K/(Wm}^{-2})$
ΔT_s^P	N/A	$\Delta T_s^P = \tilde{G}_0\Delta F^{\mathrm{TOA}} = 1.22\mathrm{K}$
ΔT_s^Γ	N/A	$\Delta T_s^\Gamma = \tilde{G}_0\tilde{g}_\Gamma\Delta F^{\mathrm{TOA}} = -0.16\ \mathrm{K}$
ΔT_s^w	N/A	$\Delta T_s^w = \tilde{G}_0\tilde{g}_w\Delta F^{\mathrm{TOA}} = 1.45\ \mathrm{K}$
$\Delta T_s^{\mathrm{tot}}$	$\Delta T_s^{\mathrm{tot}} = G\Delta F^{\mathrm{TOA}} = 2.53\ \mathrm{K}$	$\Delta T_s^{\mathrm{tot}} = \tilde{G}\Delta F^{\mathrm{TOA}} = 2.49\ \mathrm{K}$

[a] In accordance with the IPCC's climate forcing definition (Ramaswamy et al. 2001), ΔF^{TOA} is the net TOA downward radiative energy flux perturbation obtained with the stratosphere adjustment (the curve with closed circles in Fig. 1c)

Based on the TOA version of the CFRAM (TFRAM), we evaluate the partial temperature changes due to the changes in feedback agents in this simple climate model according to

$$\Delta T_s^P = \frac{\Delta F^{\mathrm{TOA}}}{(-\lambda_P)},$$
$$\Delta T_s^{\Gamma} = \frac{\sum_{m=1}^{44}\left(-\frac{\partial R^{\mathrm{TOA}}}{\partial T_m}\right)(\Delta T_m - \Delta T_s)}{(-\lambda_P)},$$
$$\Delta T_s^{w} = \frac{-\Delta^{(w)}(S-R)^{\mathrm{TOA}}}{(-\lambda_P)} \qquad (10)$$

where, $\Delta F^{\mathrm{TOA}}$is the sum of all rows in the vector $\Delta\vec{\mathbf{F}}^{\mathrm{ext}}$ defined in (5). Obviously, we use the same outputs derived from the differences between the 2 × CO_2 and 1 × CO_2 equilibrium states in the feedback analysis with both PRP and TFRAM. The products of the TFRAM are the partial changes of the surface temperature due to the external forcing alone, and due to individual feedbacks. These partial temperature changes are addable and their sum can be directly compared with the total surface temperature change between the 2 × CO_2 and 1 × CO_2 equilibrium states. The initial gain defined in the TFRAM is mathematically identical to that in the PRP and they all equal to $-1/\lambda_P$. In the TFRAM, we interpret the initial gain as the ratio between the partial temperature change due to the external forcing alone (or the temperature change when all feedbacks are suppressed) and the external forcing itself. A feedback gain in the TFRAM then is defined as the ratio of the partial temperature change due to the feedback to the partial temperature change due to the external forcing alone (e.g., $\tilde{g}_{\Gamma} = \Delta T_s^{\Gamma}/\Delta T_s^P$ and $\tilde{g}_w = \Delta T_s^w/\Delta T_s^P$). As a result, the total gain in the TFRAM is $\tilde{G} = \tilde{G}_0[1 + (\tilde{g}_{\Gamma} + \tilde{g}_w)]$. By definition, the total gains defined in both PRP and TFRAM, as the initial gain, have to be numerically identical (other than computational round-off errors) because they both are defined as the ratio of the (total) surface temperature change to the external forcing. Therefore, the net effect of the PRP feedback gains has to be numerically identical to that of the TFRAM's counterparts, namely, $[1-(g_{\Gamma}+g_w)]^{-1} = [1+(\tilde{g}_{\Gamma}+\tilde{g}_w)]$, although the feedback gains themselves of the two frameworks are defined differently and they have different numerical values, as indicated in Table 3.

5.2 TOA-only approach versus the atmosphere-surface column approach

A casual comparison between Tables 1 and 3 immediately reveals that the partial temperature changes at the surface due to the external forcing alone and due to feedbacks estimated from the TFRAM are different from those estimated from the CFRAM. Obviously, the feedbacks associated with atmospheric motions (in this model, the feedbacks associated with atmospheric motions are dry convection, surface evaporation and moist convection, and surface sensible heat flux) are absent in the TFRAM and whereas the lapse rate feedback is not defined in the CFRAM. Furthermore, the partial temperature change due to water vapor feedback, a common feedback considered in the CFRAM and TFRAM, also have different values. According to Tables 1 and 3, the surface temperature change due to water vapor feedback is equal to 2.15 K based on the CFRAM and 1.43 K based on the TFRAM.

These seemingly differences between the TFRAM and CFRAM can be resolved after accounting for the effects of non-uniform air temperature changes due to each of individual feedbacks that have been lumped into the lapse rate feedback in the TFRAM. Based on (27) in Part I, the partial surface temperature change due to the lapse rate feedback, ΔT_s^{Γ} in (10), can be rewritten as

$$\Delta T_s^{\Gamma} = \Delta T_s^{\Gamma_{\mathrm{ext}}} + \Delta T_s^{\Gamma_w} + \Delta T_s^{\Gamma_{\mathrm{dry}}} + \Delta T_s^{\Gamma_{lh}} + \Delta T_s^{\Gamma_{sh}} \qquad (11)$$

and

$$\Delta T_s^{\Gamma_{\mathrm{ext}}} = \Delta T_{44}^{\mathrm{ext}} - \Delta T_s^P; \quad \Delta T_s^{\Gamma_w} = \Delta T_{44}^{w} - \Delta T_s^{w};$$
$$\Delta T_s^{\Gamma_{\mathrm{dry}}} = \Delta T_{44}^{\mathrm{dry}}; \quad \Delta T_s^{\Gamma_{lh}} = \Delta T_{44}^{lh}; \quad \Delta T_s^{\Gamma_{sh}} = \Delta T_{44}^{sh} \qquad (12)$$

where $\Delta T_{44}^{\mathrm{ext}}$, ΔT_{44}^{w}, $\Delta T_{44}^{\mathrm{dry}}$, ΔT_{44}^{lh} andΔT_{44}^{sh} are the partial surface temperature changes calculated in the CFRAM using (7) and shown in Table 1 (the row labeled as "CFRAM"); ΔT_s^P and ΔT_s^w are given in (10) and shown in Table 3.

Equation (12) clearly illustrates that the lapse rate feedback considered in the TFRAM is equal to the total effect of the vertically non-uniform changes due to the external forcing and each of the feedbacks, including those associated with the vertical redistribution of energy by atmospheric motions that does not directly alter the TOA radiative energy flux. Table 4 lists the contributions to the surface temperature change from the uniform and non-uniform changes due to the external forcing and each of the feedbacks defined in the CFRAM. It is seen that the partial temperature change either due to a climate forcing at the

Table 4 Re-evaluations of the partial surface temperature changes in the TFRAM based on the physical and dynamical feedback processes defined in the CFRAM

	$\Delta T_s^{\mathrm{ext}}$ (K)	ΔT_s^{w} (K)	$\Delta T_s^{\mathrm{dry}}$ (K)	ΔT_s^{lh} (K)	ΔT_s^{sh} (K)	$\Delta T_s^{\mathrm{tot}}$ (K)
Uniform	1.22	1.43	0.0	0.0	0.0	2.65
Lapse rate	−0.01	0.72	0.23	−1.21	0.15	−0.12[a]
Sum	1.21	2.15	0.23	−1.21	0.15	2.53

[a] The partial surface temperature change due to the lapse rate feedback in the TFRAM is equal to −0.16 K instead of −0.12 K. The 0.04 K difference is due to the difference of the estimates of the total surface warming between the CFRAM and TFRAM

Table 5 Re-evaluations of the feedback parameters defined in the PRP method based on the physical and dynamical feedback processes defined in the CFRAM

Uniform	Lapse rate	Total (sum of the left)
N/A	$g_0^{\text{non-unif}} = \lambda_{\Gamma_{\text{ext}}}/(-\lambda_p) = -0.003$	$g_0^{\text{tot}} = -0.003$
$g_w^{\text{unif}} = 0.586$	$g_w^{\text{non-unif}} = \lambda_{\Gamma_w}/(-\lambda_p) = 0.264$	$g_w^{\text{tot}} = 0.850$
$g_{\text{dry}}^{\text{unif}} = 0.0$	$g_{\text{dry}}^{\text{non-unif}} = \lambda_{\Gamma_{\text{dry}}}/(-\lambda_p) = 0.091$	$g_{\text{dry}}^{\text{tot}} = 0.091$
$g_{lh}^{\text{unif}} = 0.0$	$g_{lh}^{\text{non-unif}} = \lambda_{\Gamma_{lh}}/(-\lambda_p) = -0.478$	$g_{lh}^{\text{tot}} = -0.478$
$g_{sh}^{\text{unif}} = 0.0$	$g_{sh}^{\text{non-unif}} = \lambda_{\Gamma_{sh}}/(-\lambda_p) = 0.059$	$g_{sh}^{\text{tot}} = 0.059$
$g_w = 0.586$(sum of the above)	$g_\Gamma = -0.067$(sum of the above)	Total feedback gain: $g^{\text{tot}} = 0.519$
Initial gain		$G_0 = 1/(-\lambda_p) = 0.257\text{K}/(\text{wm})^{-2}$
Total gain		$G = G_0(1 - g^{\text{tot}})^{-1} = 0.534K/(Wm^{-2})$

TOA or a feedback agent that influences the TOA radiation consists of two parts: a vertically uniform temperature change and an additional surface temperature change associated with the vertically non-uniform air temperature change. In this simple single column model, the only feedback that directly influences the TOA radiation energy balance is water vapor feedback. The total partial temperature change due to water vapor feedback is 2.15 K, 1.43 K coming from the uniform change and 0.72 K from the non-uniform change. The surface temperature changes due to (local) dynamic processes do not have a vertically uniform part since these dynamic processes represent energy exchange between the atmosphere and surface and have no effects directly on the TOA radiation balance. Therefore, the surface temperature changes due to (local) dynamic processes all come from the non-uniform changes.

In the PRP method, the feedbacks are measured in terms of feedback parameters instead of partial temperature changes. Again, using (27) in Part I, we obtain,

$$\lambda_\Gamma = \lambda_{\Gamma_{\text{ext}}} + \lambda_{\Gamma_w} + \lambda_{\Gamma_{\text{dry}}} + \lambda_{\Gamma_{lh}} + \lambda_{\Gamma_{sh}} \tag{13}$$

and

$$\begin{aligned} \lambda_{\Gamma_{\text{ext}}} &= \lambda_{\text{tot}} - \lambda_p \Delta T_{44}^{\text{ext}}/\Delta T_s \\ \lambda_{\Gamma_w} &= -\lambda_w - \lambda_p \Delta T_{44}^{w}/\Delta T_s \\ \lambda_{\Gamma_{\text{dry}}} &= -\lambda_p \Delta T_{44}^{\text{dry}}/\Delta T_s \\ \lambda_{\Gamma_{lh}} &= -\lambda_p \Delta T_{44}^{lh}/\Delta T_s \\ \lambda_{\Gamma_{sh}} &= -\lambda_p \Delta T_{44}^{sh}/\Delta T_s \end{aligned} \tag{14}$$

where ΔT_s is the total surface temperature change of the original climate model (2) and $\lambda_{\text{tot}} = -\Delta F^{\text{TOA}}/\Delta T_s$is the total feedback parameter of the climate model. Obviously, the sum of (14) is exactly equal to the lapse rate feedback parameter λ_Γ obtained from (9) because the feedback parameters defined in the PRP are addable to the total feedback parameter and the partial temperature changes in the CFRAM are addable to the total temperature change (other than a small error due to linearization in the PRP and CFRAM).

The combination of (14) and (9) leads to a hybrid PRP-CFRAM feedback analysis (i.e., using the PRP feedback definition but based on feedback processes defined in the CFRAM). In the hybrid PRP-CFRAM feedback analysis, each feedback gain has two parts: one is associated with the uniform change and the other is associated with the non-uniform change. Table 5 summarizes the results of the hybrid PRP-CFRAM feedback analysis. Now it becomes clear that the lapse rate feedback gain calculated in the standard PRP method is made of a collective effect of the non-uniform temperature changes due to all feedbacks present in the model. The total water vapor feedback gain is larger than the one estimated from the standard PRP method, due to the inclusion of the back radiation effect of the water vapor feedback. The evaporation and moist convection feedback is negative because it warms the atmosphere at the expense of reducing surface warming.

Because the lapse rate feedback defined in the TOA-based framework measures a collective effect of all physical and dynamical feedbacks that tend to have opposite polarity, the net lapse rate feedback is the residual of several large terms. The results shown in Tables 4 and 5 clearly indicate that the contribution to the lapse rate feedback from vertical convection is negative (this is another way of saying that evaporation feedback and moisture convection feedback tends to warm the upper atmosphere at an expense of reducing warming at the surface and lower troposphere). But changes in the atmospheric water vapor contribute to the lapse rate feedback positively. As a result of the partial cancelation between the contributions from the convection feedback and water vapor feedback, the net lapse rate feedback, although still negative, is much smaller.

Furthermore, a large part of the non-local dynamical feedback associated with poleward heat transport is also "hidden" in the lapse rate feedback in the TOA based approach. As shown in Cai (2005, 2006) and Cai and Lu (2007), an enhanced poleward heat transport causes an additional atmospheric warming in high latitudes, and the

warmer atmosphere then causes a warming amplification at the surface by emitting more radiation back to the surface below (or the "greenhouse-plus" feedback). In the TOA based analysis, part of the greenhouse-plus feedback in high latitudes is lumped together with other feedbacks in the lapse rate feedback, although the polarity change of the lapse rate feedback from negative in low latitudes to positive in high latitudes could still be suggestive of the presence of the "greenhouse-plus" feedback.

6 Summary

In Part I of the two-part series papers, we presented the formulation of a new climate feedback analysis method, namely the CFRAM (coupled atmosphere-surface climate feedback-response analysis method). The key new feature of the CFRAM is the isolation of individual contributions (or partial temperature changes) to the total temperature change of the climate system from the external forcing alone, and from each of individual physical and dynamical processes associated with the energy transfer with the space and within the climate system. Here, we demonstrate this new feature of the CFRAM and compare the CFRAM with the partial radiative perturbation (PRP) and online feedback suppression methods in the context of global warming simulations using a coupled atmosphere-surface single column climate model. In response to the external forcing due to the doubling of CO_2, the single column climate model produces a warming signal at the surface and troposphere and cooling in the stratosphere. The surface warming is 2.45 K, slightly weaker than the average tropospheric warming (about 2.7 K). The stratospheric cooling at 20 hPa is about -6 K.

We use the CFRAM to calculate the partial temperature changes due to the external forcing alone, and due to changes in water vapor (water vapor feedback), in dry convections (dry convection feedback), in evaporation and moisture convection (surface latent heat and moisture convection feedback), in surface sensible heat flux (surface sensible heat flux feedback). The last three feedbacks are (local) dynamical feedbacks reflecting changes in the vertical redistribution of energy by atmospheric motions and they do not contribute energy flux perturbations at the TOA. The calculations confirm that these partial temperature changes are addable and their sum is nearly indistinguishable from the (total) temperature change obtained from the climate simulations of the original model, except a small but noticeable difference in the stratosphere. The errors in the stratosphere result from the relatively stronger sensitivity of the longwave radiation with respect to temperature change in the upper stratosphere where the air mass in each layer in radiative transfer model is much less than that below.

The CFRAM analysis reveals that the surface warming caused by the external forcing alone is about 1.21 K. The contribution of water vapor feedback adds 2.15 K to the surface warming whereas the (local) dynamical feedback reduces the surface warming by 0.83 K, mainly due to evaporation and moist convection feedbacks that act to redistribute the excessive warming at the surface to the troposphere. Their sum (2.53 K) is very close to the actual warming in the $2 \times CO_2$ climate simulation (2.45 K). The small error at the surface ($\sim$0.08 K or less than 4%) is mainly due to linear approximations used in the radiative transfer model.

The partial temperature changes due to these feedbacks calculated using the online feedback suppression method are, although similar, numerically very different from those in the CFRAM. By definition, the partial temperature change due to a particular feedback obtained using the feedback-suppression method is the temperature difference between two different climate systems: one is the standard system with the presence of all feedbacks, and the other is a "virtual" system that include all feedbacks except the one under consideration. We apply the CFRAM to diagnose the feedbacks that are not excluded in a feedback-suppression experiment to examine what cause the differences. The calculations clearly reveal that differences between the online feedback suppression and CFRAM mainly reflect the "compensating effects" of other feedbacks in the absence of the suppressed feedback in the virtual climate system used as a reference in the online feedback suppression.

The difference in the climate feedback-response definitions in the CFRAM and PRP results in two different sets of parameters measuring climate feedbacks and their effects. To illustrate this difference, we first compare the TOA version of the CFRAM (TFRAM) with the PRP method. In the PRP method, all feedbacks are implicitly assumed to be caused by the surface temperature change. As a result, the PRP feedback parameters are additive (or all feedbacks are independent), but their effects are not, or the partial temperature changes due to individual feedback agents are not defined. In the CFRAM, the changes in all climate variables are regarded as the system responses to the external forcing and the change in the surface temperature is only part of the system responses. The other changes are regarded as "feedback agents" only because (1) the concerned climate variable in the feedback analysis is temperature and (2) the other changes contribute to energy flux perturbations, which either enhance or weaken the energy flux perturbations due to the external forcing. Under the generalized definition of climate feedback-response, the effects of the external forcing and feedbacks in the CFRAM are directly measured by the resultant "partial temperature changes". Furthermore, these partial temperature changes are addable and their sum is the (total)

temperature change in the original system. These fundamental differences are reflected in the different representations of feedback gains in the PRP and TFRAM, although both representations yield the same initial and total gains.

The other fundament difference between the PRP and CFRAM arises from the consideration of the TOA energy perturbation in the PRP versus a vertically varying energy flux perturbation in the CFRAM. In the TOA only approach, the effect of air temperature changes is considered as a feedback agent since it contributes to the change of the TOA radiative flux. We have illustrated that the lapse rate feedback parameter defined in PRP method is made of contributions from each of the physical and dynamical processes considered in the CFRAM. Specifically, the lapse rate feedback includes all effects of those feedbacks that do not contribute to energy flux perturbations at the TOA plus partial effects of those feedbacks, such as water vapor, cloud, ice-albedo feedbacks, that contribute to energy flux perturbations at the TOA. Because contributions to the lapse rate feedback from various physical and dynamical processes tend to cancel one another, the net lapse rate feedback is the residual of several large terms.

The relatively large cancelation between dominant processes in contributing the lapse rate feedback would cause some uncertainties in the estimate of the lapse rate feedback itself. This may limit the feasibility of using TOA-only feedback analysis for identifying the sources of climate projection uncertainties. For example, it is known that lapse rate feedback and water vapor feedback tend to cancel each other (Cess 1975; Held and Soden 2000; Soden and Held 2006), implying that the two feedbacks are negatively correlated. This may explain why the net effect of the water vapor and lapse rate feedbacks has a small inter-model spread despite of the fact each of the two feedbacks alone has a larger inter-model spread (Colman 2003; Soden and Held 2006). From the analysis presented in Tables 4 and 5, the negative correlation between the water vapor and lapse rate feedbacks could simply imply a negative correlation between water vapor feedback and changes in evaporation and convections. A small inter-model spread of the net effect of the water vapor and lapse rate feedbacks does not provide sufficient information about what causes larger inter-model spreads in each of the two feedbacks alone. The larger inter-model spread of the water vapor feedback could be mainly due to the partition of the water vapor feedback into the "uniform" and "non-uniform" responses. If so, this could easily cause the seeming large spreads in both water vapor and lapse rate feedbacks but a small spread in their net effect. Furthermore, the negative correlation between the strength of lapse rate feedback and ratio of the tropical warming to global warming (Soden and Held 2006) could be suggestive of either a relationship between the change in the poleward heat transport and polar warming amplification or a relationship between the change in the moisture convection in the tropics and the tropical surface warming reduction, or both. Because both the vertical convections and horizontal heat transport contribute the lapse rate feedback, we cannot isolate the dynamical factors responsible for the tropical warming reduction and polar warming amplifications based on the information provided from the lapse rate feedback. With the CFRAM, we can isolate the different roles of various physical and dynamical processes in contributing the global climate sensitivity and its spatial variations, as elucidated in Cai and Lu (2007).

Acknowledgments The authors are indebted to Dr. Qiang Fu who provided us the radiative transfer model (Fu and Liou 1993), which is the core part of the coupled atmosphere-surface single column climate model used in this study. We are grateful for constructive comments from two anonymous reviewers. This work is supported by grants from the NOAA/Office of Global Programs (GC04-163 and GC06-038).

References

Bony S et al (2006) How well do we understand and evaluate climate feedback processes? J Clim 19:3445–3482

Cai M (2005) Dynamical amplification of polar warming. Geophys Res Lett 32:L22710. doi:10.1029/2005GL024481

Cai M (2006) Dynamical greenhouse-plus feedback and polar warming amplification Part I: A dry radiative-transportive climate model. Clim Dyn 26:661–675

Cai M, Lu J-H (2007) Dynamical greenhouse-plus feedback and polar warming amplification Part II: Meridional and vertical asymmetries of the global warming. Clim Dyn 29:375–391

Cess RD (1975) Global climate change: an investigation of atmospheric feedback mechanisms. Tellus 27:193–198

Colman R (2003) A comparison of climate feedbacks in general circulation models. Clim Dyn 20:865–873

Fu Q, Liou KN (1993) Parameterization of the radiative properties of cirrus clouds. J Atmos Sci 50:2008–2025

Hall A, Manabe S (1999) The role of water vapour feedback in unperturbed climate variability and global warming. J Clim 12:2327–2346

Held IM, Soden BJ (2000) Water vapor feedback and global warming. Annu Rev Energy Environ 25:441–475

Lu J-H, Cai M (2008) A new framework for isolating individual feedback processes in coupled general circulation climate models. Part I: Formulation. Clim Dyn. doi:10.1007/s00382-008-0425-3

Manabe S, Wetherald RT (1967) Thermal equilibrium of the atmosphere with a given distribution of relative humidity. J Atmos Sci 24:241–259

Ramaswamy V et al (2001) Radiative forcing of climate change. In: Houghton JT et al (eds) Climate change 2001: the scientific basis. Cambridge University Press, Cambridge, pp 349–416

Schneider EK, Kirtman BP, Lindzen RS (1999) Tropospheric water vapor and climate sensitivity. J Atmos Sci 56:1649–1658

Soden BJ, Held IM (2006) An assessment of climate feedbacks in coupled ocean atmosphere models. J Clim 19:3354–3360

Wetherald R, Manabe S (1988) Cloud feedback processes in a general circulation model. J Atmos Sci 45:1397–1415